❏ 222

Comparison of faster region-based convolutional network for algorithms for grape leaves classification

Moechammad Sarosa[1], Puteri Nurul Ma'rifah[1], Mila Kusumawardani[1], Dimas Firmanda Al Riza[2]

[1]Department of Electrical Engineering, State Polytechnic of Malang, Malang, Indonesia
[2]Department of Biosystems Engineering, Faculty of Agricultural Technology, University of Brawijaya, Malang, Indonesia

Article Info

ABSTRACT

The shapes of leaves distinguish the Indonesian grape variants. The grape leaves might look the same at first glance, but there are differences in leaf shapes and characteristics when observed closely. This research uses a deep learning method combined with the faster region-based convolutional neural network (R-CNN) algorithm with the Inception network architecture, ResNet V2, ResNet-152, ResNet-101, and ResNet-50, and uses COCO weights trained to classify five grape varieties through leaf images. The study collected 500 images to be used as an independent dataset. The results show that network improvements can effectively improve operating efficiency. There are also limitations to training scores because the F1 score value tends to stabilize or decrease at a certain point. In the Inception ResNet V2 architecture, with the highest average F1 score of 92%, the average computing time for training and testing is longer than other network architectures. This suggests that the algorithm can classify types of grapes based on their leaves.
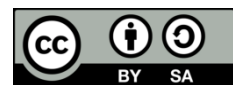
Corresponding Author:

Moechammad Sarosa
Department of Electrical Engineering, State Polytechnic of Malang
St. Soekarno-Hatta 09, Malang 65141, Indonesia
Email: msarosa@polinema.ac.id

1. INTRODUCTION

Grapes belong to the *Vitaceae* family [1], which are known to have a number of health benefits [2], [3]. It is imperative to understand the grape variant to determine the best cultivation technique, possible quality, and commercial value [4], [5]. Grape growers are working on ensuring a precise identification of grapes varieties, as well as determining how to grow cuttings based on each variety and calculating its supply price. The varieties of grapes can be distinguished on the basis of their leaf shapes [6]. Grape growers are trying to find the best way to find a precise identification of grape varieties, as well as to determine the best cultivation technique for different types of grape variants with the best commercial values. Various studies have designed different methods of classifying leaves of various types of plants over the last few years. Some of these methods are mask algorithm region-based convolutional neural network (R-CNN) and VGG16 used to distinguish leaf shapes [7], the convolutional neural network (CNN) technique [8], CNN to analyze leaf disease [9], [10], and the standard ResNet-50 CNN model's attention residual learning strategy (AResNet-50) [11].

Deep learning techniques, which help classify objects more accurately, are used by most studies to classify plant leaves. Using deep learning methods for image recognition and also classification, has widely spread in research [12]–[14]. Another classification method, CNN is one of the most common and widely used deep learning models that have been proven to have good performance due to their excellent capability of learning properties of an object using a large number of network architectures [15], [16]. Meanwhile, a new method suggested by Liu *et al.* [17], Faster R-CNN, is currently being developed. Grape leaf variants are

identified using a deep learning method with the Faster R-CNN algorithm combined with the Inception ResNet V2, ResNet-152, ResNet-101, and ResNet-50 network architecture and use pre-trained COCO weights. This research employs five types of grape leaves, namely academic, jupiter, local, taldun, and transfiguration.

2. METHOD
2.1. Research data collection
In the data collection process, images of grape leaves are taken and used to generate a dataset. The dataset contains 500 images, with 100 for each grape leaf variety. This research focuses on five grape varieties, which are academics, jupiters, local, taldun, and transfiguration. Figures 1(a) to 1(e) shows the grape leaf in one of our researchers' gardens. The resolution of the images is adjusted to the conditions set out in the preconditioning weight, namely the COCO pretrained method. The adjustment is made after collecting data on grape plant leaf images. COCO has a pre-trained weight of 640×640. Figure 1, which represents each class, shows examples of the images that are applied to this dataset. Class here refers to the type of grape variety.

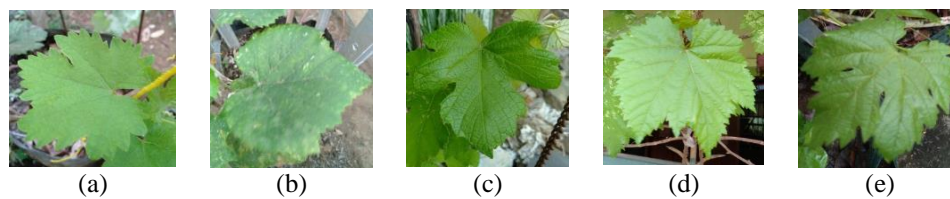| (a) | (b) | (c) | (d) | (e) |

Figure 1. Datasets (a) academic, (b) jupiter, (c) local, (d) taldun, and (e) transfiguration

2.2. Annotation and labeling
The process of marking the grape leaf in a picture is called annotation and labeling. The initial step is to draw a box on the leaf surface of the grape plant and mark each of the boxes with labels "Academic", "Jupiter", "Local", "Taldun", and "Transfiguration". A file with an extension '.xml' is generated by image annotation and labeling in the PASCAL VOC format. The annotation and labeling phase produces a baseline truth which is then used to calculate the regression loss of bounding box detection points on objects detected during training. The process employs image software. An example of the type of annotation and labeling is shown in Figure 2.
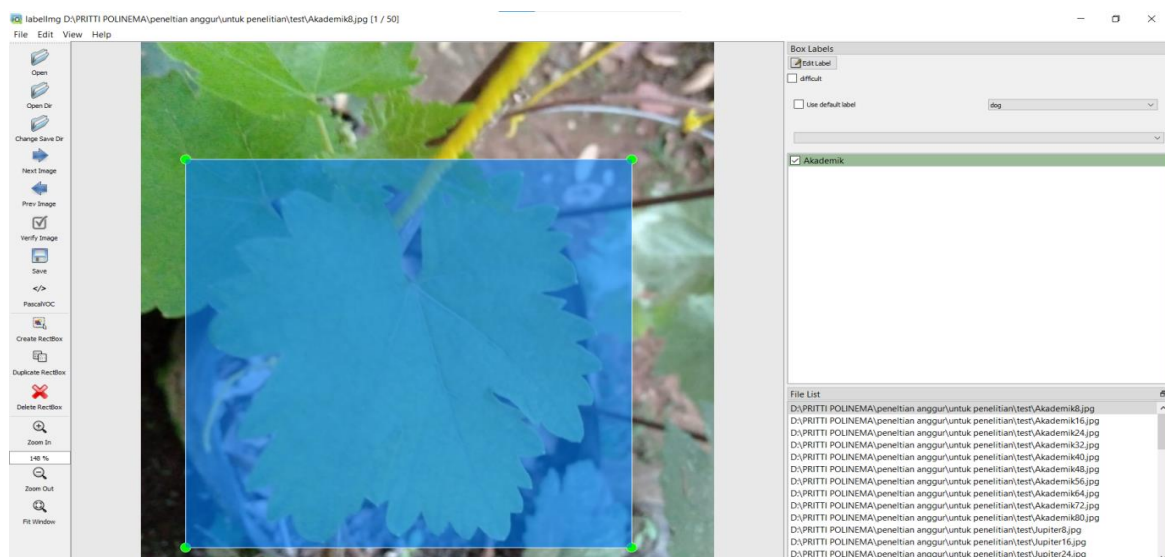

Figure 2. Labeling process using software called LabelImg

Subsequently, the data is divided into several categories, such as testing and training data, once all the images have been annotated and labeled. Table 1 shows the partition scheme for the datasets. In training, the

result of image annotation and labeling may not be directly used. To be used in training and modeling activities, the resulting annotation and label files that are generated with an extension format '.xml' have to be converted into '.csv' file formats. Table 2 illustrates the conversion results for the file to '.csv'.

Table 1. Table of dataset splits

Exp schematic-	Total training data	Total test data
1	400	50
2	450	50

Table 2. Conversion results of XML to CSV files

File name	Wide	Tall	Class	Xmin	Ymin	Xmax	Ymax
Academic5.jpg	640	640	academic	55	142	543	622
Jupiter6.jpg	640	640	jupiter	87	6	615	596
Local4.jpg	640	640	local	6	9	590	512
Taldun3.jpg	640	640	taldun	22	7	507	537
Transfiguration2.jpg	640	640	transfiguration	114	85	635	545

2.3. Modeling

Faster R-CNN is an improved CNN method that is developed from R-CNN and Fast R-CNN [18]–[20]. What sets this method apart from its predecessors is the upgrade from the selective search feature to a region proposal network (RPN) [21]. This study employs the Faster R-CNN algorithm with Inception ResNet V2, ResNet-152, ResNet-101, and ResNet-50 architecture. A modeling exercise was carried out before the experiment using Google Collaboratory tools. Figure 3 shows a model of the Faster R-CNN algorithm.
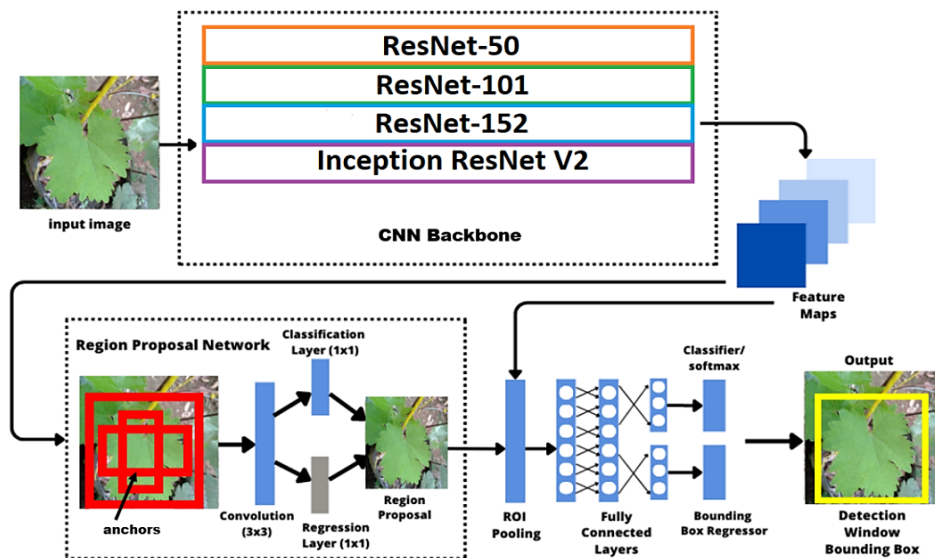

Figure 3. Model of the Faster R-CNN algorithm illustration

The Faster R-CNN architectural model begins with inputting an image and the leaf features which then are recovered using backbone CNN. The CNN known as a technology that uses a set of convolutionals to retrieve features in order [22] to create layers of care on the final result at each phase of training [23]. This method can identify the items represented in an image [24]. The research also tested the organizing capacity of COCO, computer vision, ImageNet, and natural language processing (NLP) to use large image classification data.

The CNN backbones used in this study are Inception ResNet V2, ResNet-152, ResNet-101, and ResNet-50. ResNet was one od the best deep neural networks in the 2015 classification competition know as IMAGENET large scale visual recognition competition (ILSVRC2015). ResNet-18, ResNet-50, 101, 110, 152, 164, and ResNet-1202 are all identical variants with a variable number of layers [25]. The last number in the ResNet architecture name indicates the total layers of the architecture for feature extraction in an image.

Beginning while the Inception convolution layer in ResNet V2 combines the Inception also ResNet layers, ResNet V2 is a blend of both layers. Inception ResNet V2 is a mixture of the Inception and ResNet layers, whereas the Inception convolution layer ResNet V2 is a combination of the Inception and ResNet layers [26].

The RPN, which requires future map output from a backbone network, is the next section. To display the "Anchors" set for each location in the Output feature map, RPN is performed by putting it on an input image. The anchors show different sizes and ratios of objects shown by the images. For PASCAL VOC, the anchors have three scale box sizes (128², 256², 512²) and three aspect ratios (1:1, 1:2, and 2:1), so there are nine possible anchors placed on the image input to the output feature map [27]. The output of this process determines the probability that any of the nine anchor points on the backbone feature map contains objects at that point [28].

The third part is the region of interest (ROI) polling layer, which uses a maximum polling operation to collect features from the feature map and to change their size to a fixed size. A single-dimensional feature vector containing. The ROI input for the layer that fully connected will be the polling layer's output organized as a single-dimensional feature vector. After going through the layers that fully connected, the features are also fed into the regression and classification branches in the final section, which predicts the object's correct match. This way, it is possible, for example, to generate an image of objects with the designation of bounding boxes and a possible classification result [28].

2.4. Measurement

True positive (TP), false positive (FP), and false negative (FN) values were obtained from the measurement method used to test the grape leaf classification system. FP denores that bounding box identified objects but failed to identify grape leaves, while FN indicates that the bounding box did not contain any objects in the provided figure. TP denotes that the bounding box detected grape plan leaves successfully [29], [30]. F1 scores, recall, and precision are computed using these parameters. Recall is the degree of detection success, whereas precision is the accuracy of the detection results. The F1 score was found to have a balance between recall and precision. The following formula was used to determine the F1 scores, recall, and precision [29].

$$Precision = \frac{TP}{TP+FP} \tag{1}$$

$$Recall = \frac{TP}{TP+FN} \tag{2}$$

$$F1\ Score = 2 \times \frac{Precision \times Recall}{Precision+Recall} \tag{3}$$

3. RESULTS AND DISCUSSION

3.1. Data training process computing time

The computing time is the time needed by a computer to process an algorithm and train data. Table 3 shows the training time required for each experiment. Furthermore, the Inception ResNet V2 architecture takes the longest to complete the training, while the ResNet-50 architecture has the fastest training time.

Table 3. Training process computing time

Network architecture	Experiment to-	Compute Time (minute)		
		3,000	4,000	5,000
Inception Resnet V2	1	69	69	73
	2	81	85	91
ResNet-152	1	25	31	43
	2	35	35	61
ResNet-101	1	25	31	41
	2	31	31	49
ResNet-50	1	19	29	39
	2	29	29	47

3.2. Data testing process computing time

Each network architecture for the testing process requires varying computational time depending on the complexity of the model. Testing time on the Inception ResNet V2 architecture tends to be longer compared to other architectures, with an average testing time reaching more than 100 seconds. Table 4 shows that the computational cost of the Inception ResNet V2 architecture is much higher, making it an important consideration in field applications, even though it has better performance in terms of detection accuracy.

Table 4. Testing process computing time

Network architecture	Experiment to-	Compute Time (second)		
		3,000	4,000	5,000
Inception Resnet V2	1	107	103	101
	2	101	103	101
ResNet-152	1	78	78	80
	2	80	73	73
ResNet-101	1	55	58	57
	2	58	55	65
ResNet-50	1	48	45	45
	2	44	43	42

3.3. Total loss while modeling

A key result of the modeling process for grape leaf shapes is the loss function. Weaknesses are found at every stage of the modeling process. Table 5 shows where the difference between the performances of the modeling process occurs. Regarding the average loss of the different architectures, Inception ResNet V2 shows the lowest average loss, while the average loss of ResNet-50 is the highest.

Table 5. Loss of Faster R-CNN in the modeling process

Step	Inception Resnet V2 experiment to-		ResNet-152 experiment to-		ResNet-101 experiment to-		ResNet-50 experiment to-	
	1	2	1	2	1	2	1	2
3,000	0.0872	0.0723	0.1065	0.1016	0.1375	0.1302	0.1507	0.1464
4,000	0.1052	0.0859	0.0825	0.0767	0.1232	0.1114	0.1361	0.1346
5,000	0.1096	0.1055	0.1334	0.1287	0.1398	0.1328	0.1146	0.1096
Average	0.1007	0.0879	0.1074	0.1023	0.1335	0.1248	0.1338	0.1302
Average	0.0943		0.1049		0.1291		0.1320	

3.4. True positive, false positive, and false negative test results

The TP, FP, and FN test results show the system's ability to identify and classify grape leaf objects. The test results in Table 6 on the Inception ResNet V2 architecture show a higher success rate in detecting grape leaves with higher TP values and lower FP and FN compared to other architectures. This indicates that this model is able to recognize objects more accurately, although it requires more computation time, making it a better choice for applications with high precision requirements.

Table 6. TP, FP, and FN test results

Network architecture	Experiment to-	Step	TP	FP	FN
Inception ResNet V2	1	3,000	44	5	1
		4,000	42	7	1
		5,000	42	6	2
	2	3,000	44	5	1
		4,000	44	5	1
		5,000	43	6	1
ResNet-152	1	3,000	39	9	2
		4,000	41	7	2
		5,000	40	8	2
	2	3,000	40	8	2
		4,000	42	6	2
		5,000	42	7	1
ResNet-101	1	3,000	36	11	3
		4,000	39	9	2
		5,000	39	10	1
	2	3,000	39	8	3
		4,000	41	8	1
		5,000	41	8	1
ResNet-50	1	3,000	34	13	3
		4,000	37	11	2
		5,000	39	9	2
	2	3,000	36	11	3
		4,000	38	10	2
		5,000	41	7	2

3.5. Precision, recall, and F1 score test results

The score for accuracy, recall, and F1 is calculated using the results of TP, FP, and FN in Table 6. For the Faster R-CNN architectural network models, Table 7 contains accuracy, recall, and F1 scores. Using the Faster R-CNN algorithm, the computations demonstrate the inception of ResNet V2, ResNet-152, ResNet-101, and ResNet-50 network architectural models achieve and average F1 score of 93%, 90%, 88%, and 86%, respectively. This indicates the Faster R-CNN algorithm, Inception ResNet V2 can detect and classify objects more effectively.

Table 7. Precision, recall, and F1 score test results

Network architecture	Experiment to-	Step	Precision (%)	Recall (%)	F1 score (%)
Inception ResNet V2	1	3,000	90	98	94
		4,000	86	98	91
		5,000	88	95	91
		Average			92
	2	3,000	90	98	94
		4,000	90	98	94
		5,000	88	98	92
		Average			93
		Average			92
ResNet-152	1	3,000	81	95	88
		4,000	85	95	90
		5,000	83	95	89
		Average			89
	2	3,000	83	95	89
		4,000	88	95	91
		5,000	86	98	91
		Average			90
		Average			90
ResNet-101	1	3,000	77	92	84
		4,000	81	95	88
		5,000	80	98	88
		Average			86
	2	3,000	83	93	88
		4,000	84	98	90
		5,000	84	98	90
		Average			89
		Average			88
ResNet-50	1	3,000	72	92	81
		4,000	77	95	85
		5,000	81	95	88
		Average			85
	2	3,000	77	92	84
		4,000	79	95	86
		5,000	85	95	90
		Average			87
		Average			86

3.6. Effects on F1 score results of the entire number of training steps

Figures 4(a) and 4(b) shows the effect of the total number of training steps as a function of F1 score results in both initial and subsequent trials. There is a training step limit of 3,000 steps on the Inception ResNet V2 network architecture. For ResNet-152 and ResNet-101 network architectures, the training step limit is at 4,000 steps. For ResNet 50, the limit on training steps is not yet known because the F1 score constantly rises as additional training steps are added. The overall limit of the training step is set since the F1 score tends to be stable or decreasing at a given point in the exercise.

3.7. The effects of average loss on average F1 score

Figure 5 shows the mean impact of a complete loss on an F1 score. The model is considered to perform better in examining the characteristics of an object because the general mean loss during training is lower. Hence, we can see an increase in the average F1 score. A failure to detect grape leaf type is generally due to an object being too short, undefinable, ambiguous, or due to the light affecting the image taken.

3.8. Detection results

Along with the results of the algorithm comparison that has been carried out, we made the choice to use the Faster R-CNN ResNet-101 algorithm to test the detection accuracy of grape leaf images by considering the error results during modeling, testing computing time, and the average F1 score. Figures 6(a) to 6(e) shows

an example of the detection accuracy of this research test. In addition, the image detection accuracy has reached 100%, which shows that the system is able to analyze the model accurately and detect and categorize it correctly. Detection error due to the dataset not being varied and the lighting when taking the picture.
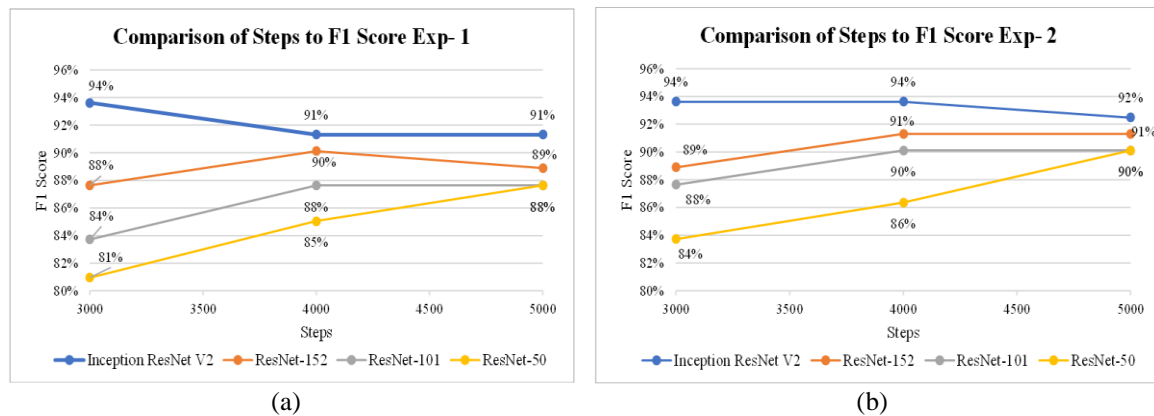

(a)   (b)

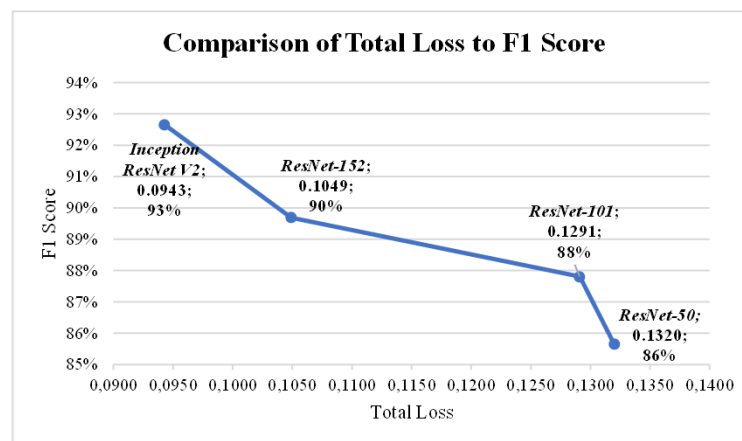Figure 4. Effects of training on the F1 score (a) first trial and (b) second trial

Figure 5. The effect of average loss on average F1 score

(a)   (b)   (c)   (d)   (e)
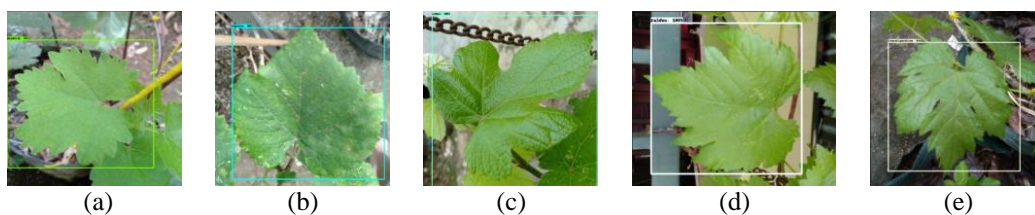
Figure 6. Detection results of (a) academic, (b) jupiter, (c) local, (d) taldun, and (e) transfiguration

4. CONCLUSION

This study describes techniques for classifying and making use of the Faster R-CNN algorithm to identify grape leaves also with the ResNet V2, ResNet-152, ResNet-101, and ResNet-50 network architectures, all of which serve as trained networks for feature extraction. The experiment results show that the average F1 scores are 93%, 90%, 88%, and 86% respectively, with the best F1 score on the Inception ResNet V2 network architecture (an average loss of 0.943). However, the time needed for training and testing is far more intensive than the other network architectures. While the architecture with the fastest computing time for

training or testing is the ResNet-50 network architecture, the F1 score of this architecture is the lowest compared to others. Furthermore, the training step limit for the Inception ResNet V2 is at step 3,000, while ResNet 152 and ResNet-101 network architectures have 4,000 step training step limit. Meanwhile, the training step limit for the ResNet-50 architecture, given that the F1 score continues to increase as the exercise step increases, is unknown. The research establishes a general limit on the number of training steps as the F1 score tends to stabilize or decline at some point during an exercise. It can be concluded that the Faster RCNN-based detection and classification system for grape leaf can analyze object properties more effectively if total losses during training are lowered.

ACKNOWLEDGEMENTS

REFERENCES

[1] M. Sarosa, P. N. Maa'rifah, M. Kusumawardani, and D. F. Al Riza, "*Vitis Vinera L.* leaf detection using faster R-CNN," *BIO Web Conference*, vol. 117, pp. 1–9, 2024, doi: 10.1051/bioconf/202411701021.

[2] A. Rahemi, J. C. D. Peterson, and K. T. Lund, "Grape Species," in *Grape Rootstocks and Related Species*, Springer, Cham, 2022, pp. 5–21, doi: 10.1007/978-3-030-99407-5_2.

[3] A. M. Walker, C. Heinitz, S. Riaz, and J. Uretsky, "Grape taxonomy and germplasm," in *The Grape Genome*, Springer, Cham, 2019, pp. 25–38, doi: 10.1007/978-3-030-18601-2_2.

[4] G. Hasanaliyeva *et al.*, "Effects of production region, production systems and grape type/variety on nutritional quality parameters of table grapes; results from a UK retail survey," *Foods*, vol. 9, no. 12, 2020, doi: 10.3390/foods9121874.

[5] B. Suter, A. D. Irvine, M. Gowdy, Z. Dai, and C. V. Leeuwen, "Adapting wine grape ripening to global change requires a multi-trait approach," *Frontiers in Plant Science*, vol. 12, pp. 1–17, 2021, doi: 10.3389/fpls.2021.624867.

[6] Y. Khan *et al.*, "Antioxidant potential in the leaves of grape varieties (*Vitis vinifera L.*) grown in different soil compositions," *Arabian Journal of Chemistry*, vol. 14, no. 11, 2021, doi: 10.1016/j.arabjc.2021.103412.

[7] K. Yang, W. Zhong, and F. Li, "Leaf segmentation and classification with a complicated background using deep learning," *Agronomy*, vol. 10, no. 11, 2020, doi: 10.3390/agronomy10111721.

[8] N. A. Othman, N. S. Damanhuri, N. M. Ali, B. C. C. Meng, and A. A. A. Samat, "Plant leaf classification using convolutional neural network," *2022 8th International Conference on Control, Decision and Information Technologies (CoDIT),* Istanbul, Turkey, pp. 1043–1048, 2022, doi: 10.1109/CoDIT55151.2022.9804121.

[9] J. Hang, D. Zhang, P. Chen, J. Zhang, and B. Wang, "Classification of plant leaf diseases based on improved convolutional neural network," *Sensors*, vol. 19, no. 19, pp. 1–14, 2019, doi: 10.3390/s19194161.

[10] Y. Toda and F. Okura, "How convolutional neural networks diagnose plant disease," *Plant Phenomics*, vol. 2019, 2019, doi: 10.34133/2019/9237136.

[11] A. Pandey and K. Jain, "Plant leaf disease classification using deep attention residual network optimized by opposition-based symbiotic organisms search algorithm," *Neural Computing and Applications*, vol. 34, pp. 21049–21066, 2022, doi: 10.1007/s00521-022-07587-6.

[12] P. N. Ma'rifah, M. Sarosa, and E. Rohadi, "Garbage classification using Faster R-CNN," *2023 International Conference on Electrical and Information Technology (IEIT),* Malang, Indonesia, pp. 196–201, 2023, doi: 10.1109/IEIT59852.2023.10335519.

[13] Q. Lv, S. Zhang, and Y. Wang, "Deep learning model of image classification using machine learning," *Advances in Multimedia*, vol. 2022, 2022, doi: 10.1155/2022/3351256.

[14] Z. Li *et al.*, "A high-precision detection method of hydroponic lettuce seedlings status based on improved Faster RCNN," *Computers and Electronics in Agriculture*, vol. 182, 2021, doi: 10.1016/j.compag.2021.106054.

[15] M. M. Taye, "Theoretical understanding of convolutional neural network : concepts, architectures, applications, future directions," *Computation*, vol. 11, no. 52, 2023.

[16] X. Wang, Y. Zhao, and F. Pourpanah, "Recent advances in deep learning," *International Journal of Machine Learning and Cybernetics*, vol. 11, no. 4, pp. 747–750, 2020, doi: 10.1007/s13042-020-01096-5.

[17] S. Liu, H. Ban, Y. Song, M. Zhang, and F. Yang, "Method for detecting Chinese texts in natural scenes based on improved faster R-CNN," *International Journal of Pattern Recognition and Artificial Intelligence*, vol. 34, no. 2, 2020, doi: 10.1142/S021800142053002X.

[18] L. Jiang, J. Chen, H. Todo, Z. Tang, S. Liu, and Y. Li, "Application of a Fast RCNN based on upper and lower layers in face recognition," *Computational Intelligence and Neuroscience*, vol. 2021, 2021, doi: 10.1155/2021/9945934.

[19] P. N. M. Ma'rifah, M. Sarosa, and E. Rohadi, "Comparison of Faster R-CNN ResNet-50 and ResNet-101 methods for recycling waste detection," *International Journal of Computer Applications Technology and Research*, vol. 12, no. 12, pp. 26–32, 2023, doi: 10.7753/ijcatr1212.1006.

[20] W. Liu, S. Liao, W. Hu, X. Liang, and X. Chen, "Learning efficient single-stage pedestrian detectors by asymptotic localization fitting," *Proceedings of the European Conference on Computer Vision (ECCV)*, pp. 643–659, 2018, doi: 10.1007/978-3-030-01264-9_38.

[21] W. Zou, Z. Zhang, Y. Peng, C. Xiang, S. Tian, and L. Zhang, "SC-RPN: A strong correlation learning framework for region proposal," *IEEE Trans. Image Process.*, vol. 30, pp. 4084–4098, 2021, doi: 10.1109/TIP.2021.3069547.

[22] L. Fan, T. Zhang, and W. Du, "Optical-flow-based framework to boost video object detection performance with object enhancement," *Expert Systems with Applications*, vol. 170, 2020, 2021, doi: 10.1016/j.eswa.2020.114544.

[23] A. Ajit, K. Acharya, and A. Samanta, "A review of convolutional neural networks," *2020 International Conference on Emerging Trends in Information Technology and Engineering (ic-ETITE),* Vellore, India, pp. 1–5, 2020, doi: 10.1109/ic-ETITE47903.2020.049.

[24] J. Li *et al.*, "Automatic detection and classification system of domestic waste via multimodel cascaded convolutional neural

network," *IEEE Transactions on Industrial Informatics*, vol. 18, no. 1, pp. 163–173, 2022, doi: 10.1109/TII.2021.3085669.

[25] L. Ichim and D. Popescu, "Melanoma detection using an objective system based on multiple connected neural networks," *IEEE Access*, vol. 8, pp. 179189–179202, 2020, doi: 10.1109/ACCESS.2020.3028248.

[26] J. Wang, X. He, S. Faming, G. Lu, H. Cong, and Q. Jiang, "A real-time bridge crack detection method based on an improved Inception ResNet V2 structure," *IEEE Access*, vol. 9, pp. 93209–93223, 2021, doi: 10.1109/ACCESS.2021.3093210.

[27] Y. P. Chen, Y. Li, and G. Wang, "An enhanced region proposal network for object detection using deep learning method," *PLoS One*, vol. 13, no. 9, pp. 1–26, 2018, doi: 10.1371/journal.pone.0203897.

[28] W. Gu *et al.*, "High accuracy thyroid tumor image recognition based on hybrid multiple models optimization," *IEEE Access*, vol. 8, pp. 128426–128439, 2020, doi: 10.1109/ACCESS.2020.3008401.

[29] N. A. Prasetyo, Pranowo, and A. J. Santoso, "Automatic detection and calculation of palm oil fresh fruit bunches using faster R-CNN," *International Journal of Applied Science and Engineering*, vol. 17, no. 2, pp. 121–134, 2020, doi: 10.6703/IJASE.202005_17(2).121.

[30] M. Sarosa, N. Muna, and E. Rohadi, "Performance of faster R-CNN to detect plastic waste," *International Journal of Advanced Trends in Computer Science and Engineering*, vol. 9, no. 5, pp. 7756–7762, 2020, doi: 10.30534/ijatcse/2020/120952020.

BIOGRAPHIES OF AUTHORS

Moechammad Sarosa received the diploma of engineering technology from Universite de Nancy I, France in 1989. He obtained his master's and doctoral degrees from Bandung Institute of Technology, Indonesia in 2002 and 2007 respectively. He has been the recipient of several research grants funded by the Ministry of Research, Technology and Higher Education of the Republic of Indonesia. His current research interests lie in information and communication technology, artificial intelligence, mobile computing, and IoT. He can be contacted at email: msarosa@polinema.ac.id.

Puteri Nurul Ma'rifah completed Diploma studies in Telecommunications and Master of Electrical Engineering concentration in Telecommunication Science and Information Technology at the State Polytechnic of Malang. In 2020 it passed the 33rd PIMNAS in the field of Community Service Research, and in 2023 received a Master's Thesis Research grant from the Ministry of Education, Culture, Research, and Technology. While studying masters, he has become a teaching assistant helping teach digital image processing and artificial intelligence workshop courses, after graduating from the master's degree involved in research at the Integrated Applied Technology Research Center (PRITTI) State Polytechnic of Malang. She can be contacted at email: pnurulmarifah@gmail.com.

Mila Kusumawardani received the M.T. degree in Electro Engineering from Brawijaya University of Malang, Indonesia, in 2010. She is a lecturer in Digital Telecommunications Networks Study Program of Electrical Engineering Department of State Polytechnics of Malang. She can be contacted at email: mila.kusumawardani@polinema.ac.id.

Dimas Firmanda Al Riza got a Doctoral degree from Kyoto University, Japan in the field of Bio-sensing Engineering in 2019. The doctoral study was completed with the LPDP presidential scholarship. He has published more than 70 scientific papers until 2022 including dozens of them in Q1 reputable international journals. Recently, he received Young Researcher's Academic Encouragement Award 2021 from The Japanese Society of Agricultural Machinery and Food Engineers (JSAM). Currently, he is the Head of the Mechatronics Laboratory of Agro-industry Tools and Machinery, Department of Agricultural Engineering, Faculty of Agricultural Technology, Universitas Brawijaya. He can be contacted at email: dimasfirmanda@ub.ac.id.